Eleven-year solar cycle signal throughout the lower atmosphere

K. Coughlin and K. K. Tung

Department of Applied Mathematics, University of Washington, Seattle, Washington, USA

Received 6 April 2004; revised 13 July 2004; accepted 5 August 2004; published 6 November 2004.

[1] A statistically significant atmospheric signal, which represents the influence of solar radiation changes on our climate, is found in global data (1958–2003). Using a nonlinear, nonstationary time series analysis, called empirical mode decomposition, it is shown that atmospheric temperatures and geopotential heights are composed of five global oscillations and a trend. The fourth mode is synchronized with the 11-year solar flux almost everywhere in the lower atmosphere. Statistical tests show that this signal is different from noise, indicating that there is enhanced warming in the troposphere during times of increased solar radiation. *INDEX TERMS:* 1610 Global Change: Atmosphere (0315, 0325); 1650 Global Change: Solar variability; 3309 Meteorology and Atmospheric Dynamics: Climatology (1620); *KEYWORDS:* solar cycle, climate signals

Citation: Coughlin, K., and K. K. Tung (2004), Eleven-year solar cycle signal throughout the lower atmosphere, *J. Geophys. Res.*, *109*, D21105, doi:10.1029/2004JD004873.

1. Introduction

[2] In order to isolate anthropogenic effects on our climate, such as warming by greenhouse gases, we must also understand the natural variability of our atmosphere. Here we show that the low-frequency variability of the region directly related to the surface climate, the troposphere, can be described in terms of five oscillations and a trend. The fourth mode in this analysis has an average period of 11 years and indicates enhanced thermal warming during times of maximum solar radiation. We use the longest global data set available (National Centers for Environmental Prediction/National Center for Atmospheric Research (NCEP/NCAR) reanalysis from 1958 to 2003), which now spans four solar cycles. Over each 11-year solar cycle the total energy output of the Sun varies by about 0.1% and its ultraviolet radiation fluctuates by 6–8%, with higher irradiance values during solar maxima than during solar minima [*Willson and Hudson*, 1988; *Lean et al.*, 1997; *Haigh*, 2002]. Since 1795 it has been speculated that these variations influence our climate [*Hershel*, 1801]. Accumulated observational [*Frederick*, 1977; *Labitzke*, 1982; *Crowley and Kim*, 1996; *Labitzke and van Loon*, 1995; *McCormack and Hood*, 1996; *van Loon and Labitzke*, 1998; *Haigh*, 2002; *Labitzke et al.*, 2002; *Gleisner and Thejll*, 2003] and modeling [*Wetherald and Manabe*, 1975; *Baldwin and Dunkerton*, 1989; *Hamilton*, 1990; *Kodera*, 1993; *Rind and Overpeck*, 1993; *Balachandran and Rind*, 1995; *Naito and Hirota*, 1997; *Haigh*, 1999; *Shindell et al.*, 1999; *Soukharev*, 1999; *Tett et al.*, 1999; *Salby and Callaghan*, 2000; *Soukharev and Hood*, 2001; *Kuroda and Kodera*, 2002] studies point to the existence of a 10- to 12-year oscillation associated with changes in the solar radiation. Because the potential signal associated with the 11-year solar cycle is likely small in amplitude and varies over a relatively long period of time compared with other climate signals with larger variance, it is difficult to detect and even more difficult to prove as being statistically significant. As pointed out by *Pittock* [1978], some of the earlier pitfalls in the statistical analyses of this signal include the following: assuming each year in the time series to be independent, failing to appreciate the effect of autocorrelation or smoothing on significant testing, and selecting a posteri the most favorable regional results for statistical analysis from a global map. We therefore pay particular attention to these issues in the present analysis. We have shown elsewhere [*Coughlin and Tung*, 2004] that the interval between independent points, in our analysis, should be about 5 years for the purpose of determining the number of degrees of freedom for the solar cycle signal. We will show that our signal is global and ubiquitous by demonstrating that various near-global means are statistically significant and that individual latitudinal strips of 20° at each pressure level share the same property (with the exception of South Polar latitudes, where the data quality may be less than desired). Our statistical analyses will include the observed autocorrelation of the atmospheric data under consideration. However, because we need global data of sufficient quality, the 45 years of data available to us consist of only four solar cycles, perhaps one to two cycles short compared with the optimal length suggested by Pittock. Nevertheless, we show that this length is sufficient according to our analysis, if the data record is not further sorted according to atmospheric phenomena, such as the phase of the quasi-biennial oscillation (QBO). Since volcanic aerosols can warm or cool the atmosphere, there is also a concern that volcanic eruptions can contaminate the solar cycle signal [*Graf et al.*, 1993; *Haigh*, 1999; *Lee and Smith*, 2003]. Of particular concern are the eruptions of El Chichon in 1982 and Pinatubo in 1991, coincidentally occurring during the two previous solar

0148-0227/04/2004JD004873$09.00

maxima. In the troposphere, however, volcanic effects tend to cool the atmosphere [*Ramanathan*, 1988; *Dutton and Christy*, 1992]. Their contribution is therefore opposite to the observed effect of increased solar radiation. Despite the fact that these two major eruptions have occurred during solar max conditions, our results still show that the troposphere is warmer during times of maximum solar radiation.

[3] Tropospheric temperatures have previously been compared to solar variability in a number of ways. *Crowley and Kim* [1996] used the length of the solar cycles as well as solar activity to show that the annual mean temperatures in the Northern Hemisphere were correlated to solar variability. *Labitzke* [1982] used zonally averaged annual temperatures to show that there are positive correlations (though low in the troposphere) with the 10.7 cm solar flux over all latitudes [*Labitzke et al.*, 2002]. *van Loon and Shea* [1999, 2000] used 3-year running seasonal means and showed that although the Northern Hemisphere temperatures are positively correlated with the solar flux, the effect seems to change with the seasons, latitudes and longitudes considered. We find, however, that the spatial structure of the correlations are sensitive to the averaging period. With increased analysis it becomes obvious that it is not just seasonality and spatial distributions of the solar signal itself but mainly contamination of this small signal by other large signals in the atmosphere that causes difficulty in analyzing and substantiating the solar signal.

[4] We have decided against using subjective methods such as Fourier analysis for detecting the solar cycle. Fourier analysis is subjective because it assumes a priori that the signal should have a constant period and a constant amplitude throughout the length of the time series. Neither of these assumptions is applicable to the solar cycle index or to the atmospheric signal correlated with it. This has the potential effect of reducing the amplitude of the extracted signal. Given that our length of record is already short, the statistical significance of the signal cannot be demonstrated at all pressure levels. Figure 1 shows the Fourier spectra of the 600-hPa geopotential height (January 1948 to February 2004) data averaged from 20° to 90°N. The statistics are naively calculated, with the mean (magenta line) fitted to the spectra of the data without the annual cycle and the 95% confidence interval calculated with a student t test. In Figure 1, there is a Fourier spectral peak near the 11-year period. Its amplitude is reduced from that of the "true" signal because of its entanglement with other atmospheric signals. This Fourier signal is also difficult to see everywhere over the globe. At 700 hPa, there is less noticeable power at 11 years, and when only the years after 1958, where the data are considered more reliable, are used, the power at this period also diminishes. The statistics calculated here do not take into consideration the choice of height or the choice of years included in the spectrum. This would also diminish the significance of the signal. A more objective method should be one which can disentangle the atmospheric signals from one another.

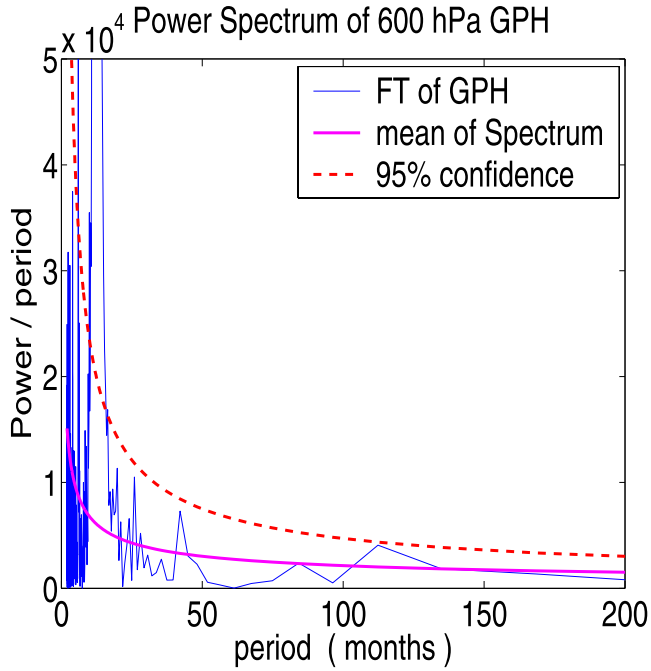

Figure 1. The Fourier transform (FFT) spectra of the 600-hPa geopotential height (GPH) (January 1948 to February 2004) averaged from 20° to 90°N. The mean (magenta line) is fitted to the spectra without the annual cycle, and the 95% confidence interval is calculated using a student t test. The degrees of freedom are calculated by $N^* = -\frac{N}{2}\log(\rho)$, where ρ is the autocorrelation of the time series minus climatology, 0.60. Power/period is plotted per period so that the area under the curve conserves power.

Figure 2. (a) Decomposition of National Centers for Environmental Prediction/National Center for Atmospheric Research (NCEP/NCAR) reanalysis geopotential height for the period of January 1958 to December 2003 at 700 hPa from 10°N to 30°N. Total height (in meters) is decomposed into five modes (intrinsic mode functions (IMF)) and a trend. The correlation between the fourth mode and the 10.7-cm solar flux is 0.72. (b) Decomposition of NCEP/NCAR reanalysis temperatures at 600 hPa from 70°N to 90°N. Total temperature (in °C) is decomposed into five modes and a trend. The correlation between the fourth mode and the 10.7-cm solar flux is 0.72. (c) Decomposition of NCEP/NCAR reanalysis geopotential height for the period of January 1958 to February 2004 at 500 hPa from 20°N to 90°N zonally and spatially averaged. Total height (in meters) is decomposed into five modes and a trend. The correlation between the fourth mode and the solar flux is 0.62. (d) A Monte Carlo–type test of significance. The 700-hPa climatology is added to 500 autocorrelated time series to generate a Monte Carlo test. The red noise is calibrated using the difference between the first mode and the climatology [*Coughlin and Tung*, 2004], and the autocorrelation of the noise is the same as the autocorrelation of the 700-hPa geopotential height anomalies, 0.54. These time series are decomposed using the empirical mode decomposition method, and the average power in modes 2, 3, and 4 of each of the decompositions is plotted Figure 2d. The solid blue line represents the linear least squares fit of these points, and the red line is two standard deviations from the best fit line. The average powers of IMFs 2, 3, and 4 of the 700-hPa geopotential heights are plotted as stars and clearly lie above the random noise level.

[5] Multiple regression analysis is one way to separate the signals. *Gleisner and Thejll* [2003] used multiple regression analysis on annual mean temperatures to disentangle the atmospheric signals. Their multiple regression includes not only the solar cycle, but also El Niño–Southern Oscillation (ENSO), a trend and volcanic signals. *Haigh* [2002] includes these as well as other signals in her multiple regressions, notably the quasi-biennial oscillation of the equatorial winds, and she recovers a different structure of solar influence. Since the solar cycle response is dependent on the choice of other signals used in the multiple regression analysis, it is important to find an objective way to disentangle the atmospheric signals. The determination of spatial and temporal structures of the atmospheric response to the solar cycle involves more than correlating filtered atmospheric data with a solar cycle index. First, we should establish the existence and structure of atmospheric modes without reference to the solar cycle or other preconceived notions of influence. Then we can ask whether the atmospheric modes are correlated with the solar cycle. So, we are faced with the issue of not just finding a

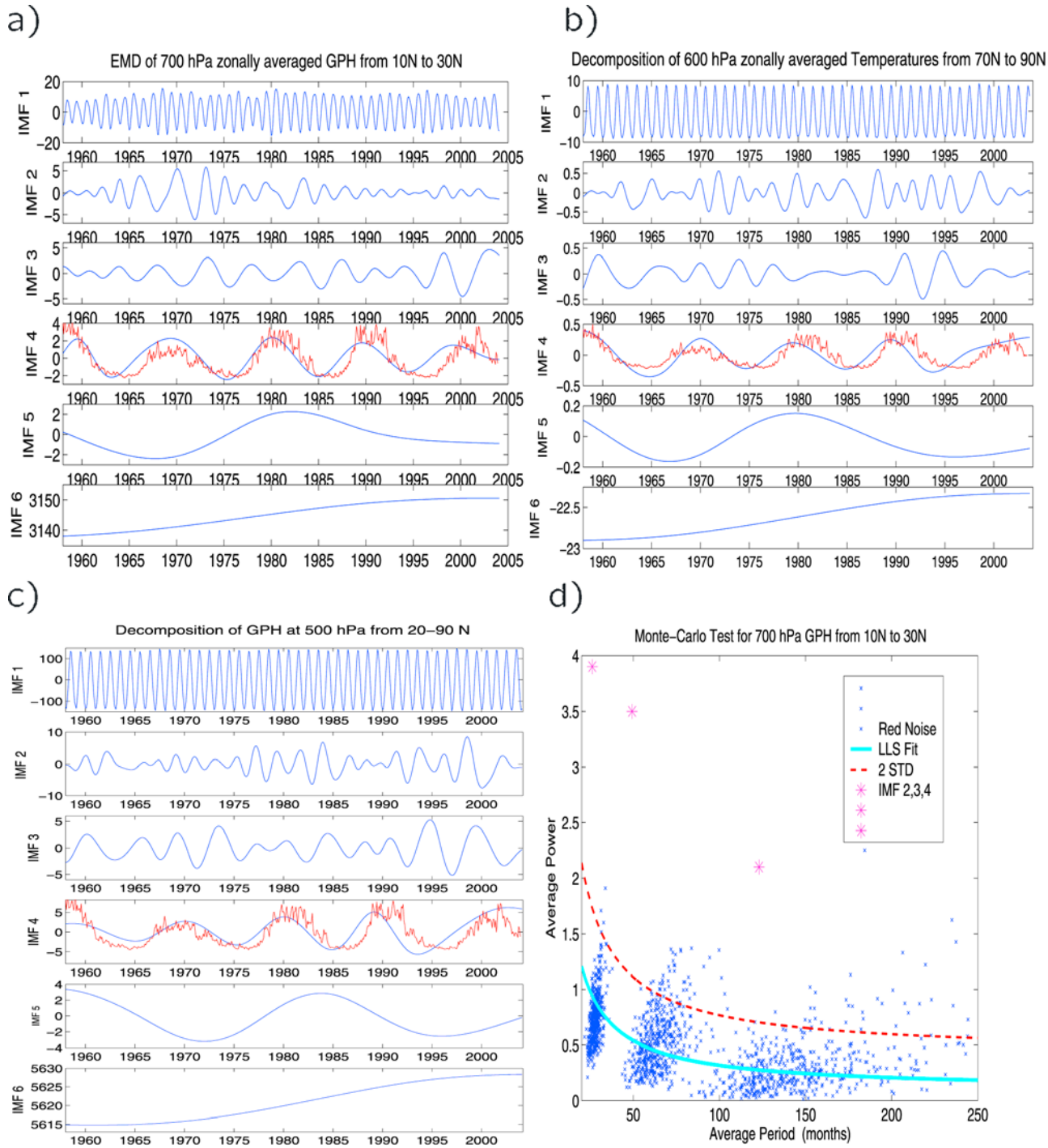

Figure 2

signal which has a decadal period but finding a signal which is correlated with the solar flux and is a statistically viable atmospheric signal itself.

2. Procedure

[6] Using empirical mode decomposition (EMD), we are able to take into account other atmospheric signals without having to guess what they are before the analysis. This method separates time series into intrinsic oscillations using the local temporal and structural characteristics of the data. In this way, the major modes are accounted for and each atmospheric signal is locally independent, thus less contaminated by the others. Our analysis also allows us to describe the statistical confidence of our results. We use monthly mean geopotential heights and temperatures [*Kalnay et al.*, 1996] from 1000 hPa to 10 hPa, and from January 1958 to December 2003. At each height the total temperature and geopotential height is subdivided into area-weighted overlapping latitudinal strips of 20°, with 10° strips near the equator. The time series of each of these strips is decomposed into locally orthogonal modes using the EMD method [*Huang et al.*, 1998]. As an example, Figures 2a and 2b show typical decompositions. Figure 2a shows temporal modes of the total geopotential height at 700 hPa averaged from 10°N to 30°N and Figure 2b shows the decomposition of the total temperature at 600 hPa averaged from 70°N to 90°N. Figure 2c shows the decomposition of the average geopotential height in the Northern Hemisphere (from 20°N to 90°N) at 500 hPa. It too contains these same five modes and a trend. The results for all 17 levels of the NCEP/NCAR reanalysis show similar decompositions consisting of only five modes, each with a variable amplitude and period, and a trend. The fact that the decompositions are so similar indicates that these signals are ubiquitous. The modes, defined by the EMD method, are called intrinsic mode functions (IMFs).

[7] To determine the statistical significance of these "intrinsic" modes we compare the power in each mode to the power in multiple decompositions of red noise spectra using a Monte Carlo type method. Taking into account the natural correlation of atmospheric data, 500 time series are randomly generated with the same autocorrelation as each real time series. Details of this technique are described by *Coughlin and Tung* [2004]. The noise spectrum for the data in Figure 2a is shown in Figure 2d with the average power of the atmospheric modes 2, 3, and 4 marked with stars. Since the power in each of the atmospheric modes is well above the noise level, Figure 2d indicates that they contain significant signals. Similar results are found at the other tropospheric heights and latitudes, indicating that these IMFs are statistically different from noise. To demonstrate that the 11-year mode is not dependent on the previous modes in the decomposition, or the result of period doubling, we remove a Fourier representation of the QBO signal from the data and then reapply the EMD. The 11-year signal remains, indicating that it is ubiquitous.

[8] Once the modes are shown to be significant internal oscillations of the atmospheric time series, correlations can be calculated between the modes and related phenomena to determine their physical significance. The first IMF is the annual cycle, with an average period of 12 months. The second mode has an average period of 28 months and is

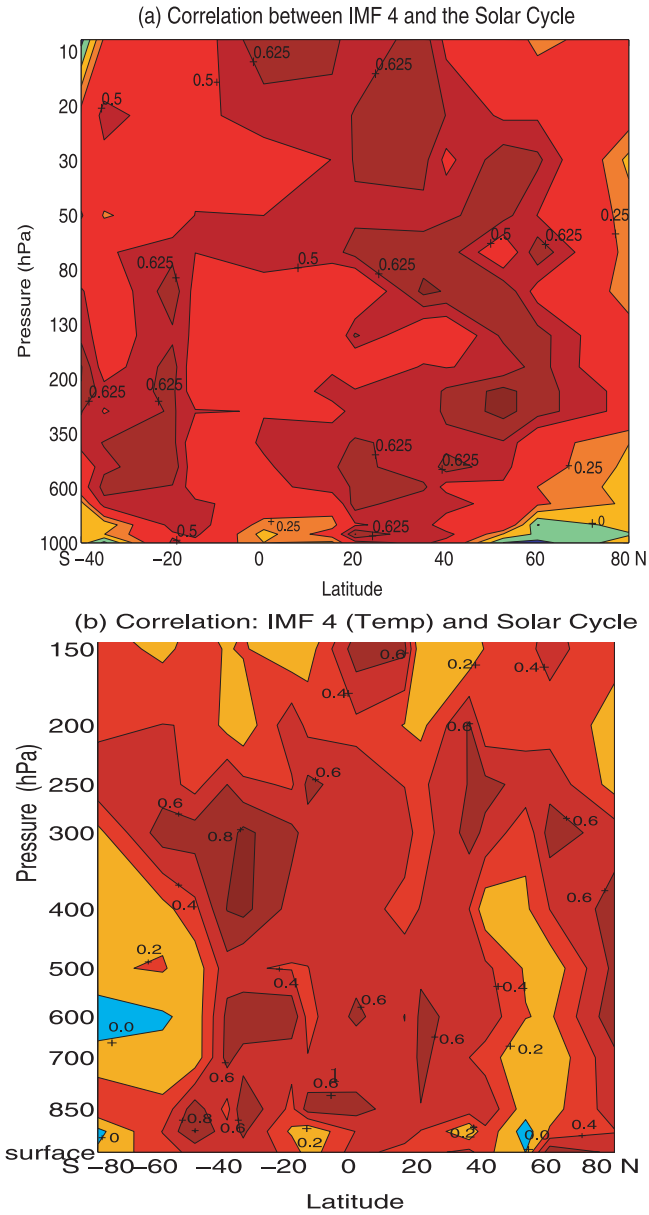

Figure 3. (a) Correlation coefficients between the fourth mode of geopotential height and the solar flux from the surface (1000 hPa) to the stratosphere (10 hPa). The coefficients are plotted at the pressure altitude and mean latitude of each decomposition. (b) A map of correlation coefficients between the fourth mode of latitudinal strips of temperature and the solar flux from the surface (surface temperatures) to 100 hPa. The coefficients are plotted at the pressure altitude and mean latitude of each decomposition. Contours indicate correlations changes of 0.2.

associated with the equatorial QBO in the stratosphere. The third mode is positively correlated with the multivariate El Niño/Southern Oscillation (ENSO) index in the tropics, and anticorrelated near the surface between 40°N and 60°N. The fourth mode has an average period of 11 years. It is highly correlated with the 10.7 cm solar flux. In the first two examples (Figures 2a and 2b), the correlation coefficient of the fourth mode with the 10.7-cm solar flux is 0.72 and the change in amplitude between solar maxima and solar minima

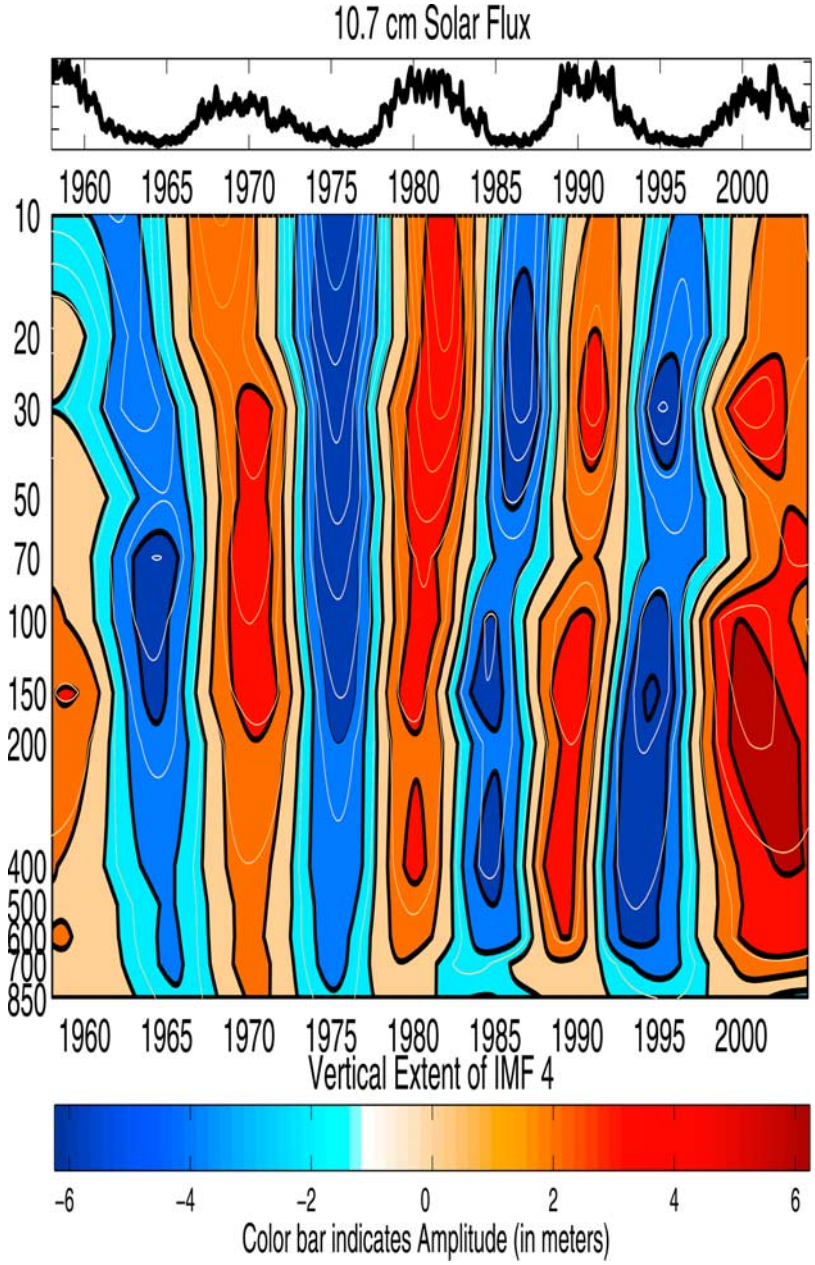

Figure 4. The fourth IMF of the spatially average Northern Hemisphere (from 20° to 90°N) geopotential height from 10 hPa down to 850 hPa. The colors indicated the strength of the signal over time, where red values are positive and blue values are negative. The magnitudes (in meters) are normalized by $\sqrt{\text{pressure}/700\text{hPa}}$ so that at 700 hPa, they also represent the true amplitudes. The true magnitude of IMF 4 is also indicated at every level by the white contour lines, spaced at 5-m intervals. A thin bar above the contour plot shows the solar flux over time. Notice that the sunspots correlate well with the fourth IMF throughout the troposphere and lower stratosphere.

is about 5 m at 700 hPa and 0.7°C at 600 hPa. We refrain from commenting on the fifth mode since the data record contains only two periods of this oscillation. The nonlinear trend indicates warming in the troposphere in recent decades. A similar result at 30 hPa in the lower stratosphere has been shown by *Coughlin and Tung* [2004], except that the secular trend in the stratosphere indicates cooling. These trends are consistent with the anticipated effect of increasing greenhouse gases. Here we focus on the fourth mode and its relation to the solar flux. Results of the correlations between the 11-year temperature mode and the 10.7-cm solar flux are calculated for the decomposition of each latitudinal strip from 1000 hPa to 150 hPa. Figure 3a shows the correlations between the solar flux and the fourth mode of geopotential height and the correlation values.

3. Results

[9] The solar flux is positively correlated with the fourth modes in temperature and geopotential height almost

everywhere, with the exception of a few decompositions where the correlations are small and not significant (see Figures 3a and 3b). In the South Hemisphere poleward of 40°S, where the data quality is known to be poor, low correlations are found. There is also a narrow strip at 50°N with low temperature correlations. These correlations, however, do not indicate a reversal of the relationship or a change in amplitude. A closer inspection of the time series in these areas of low correlations reveals that the signal is not regular enough to produce a statistical connection. Only with more time can the relationship between the signal and the solar flux be established in these areas. However, in many places the correlations are large enough to demonstrate a high statistical relationship (correlations above 0.58 are statistically significant at the 95% level using a student *t* test with independent data points every 5 years), and the overwhelming picture is that of a positive correlation between the solar flux and this mode throughout the troposphere.

[10] Previously, we showed that the 11-year solar cycle is statistically correlated with dynamical variables in the stratosphere [*Coughlin and Tung*, 2004]. Here we demonstrate (in Figure 3) that the fourth atmospheric mode in the troposphere is correlated with the 11-year solar cycle. Figure 4 shows the fourth mode in geopotential height at 15 levels (from 850 hPa up to 10 hPa). Not only is the mode vertically coherent throughout the stratosphere and troposphere, but it is also approximately synchronous with the solar flux shown in the horizontal strip at the top of Figure 4. In Figure 4, the amplitudes of the fourth mode of the average Northern Hemisphere geopotential heights are scaled by the square root of the pressure (or analogously the density) in order to display the mode compactly. The signals increase with height from about 5 m in the troposphere to more than 70 m in the stratosphere. The white contour lines, indicate the actual amplitudes at intervals of 5 m. The overall picture demonstrates the ubiquitous nature of this fourth mode and its coherence with the solar flux. However, on a finer scale (i.e., looking at smaller spatial averages), the amplitude and timing of the fourth mode is not as consistent. This is probably due to the presence of high natural variability in the atmosphere close to the surface. This is reduced with spatial averaging. Our analysis produces amplitudes consistent with the composite differences, between solar maxima and minima, of the annual mean geopotential height found by *Labitzke et al.* [2002]. They found peak-to-peak differences of 5 m at the surface increasing up to 100 m at 10 hPa. Compared to their results our correlation coefficients in the troposphere are higher (see Figure 3). Our results are also statistically significant and we find consistent timing and amplitudes throughout the troposphere.

4. Conclusion

[11] Through this EMD representation, we are able to see the natural variations in the atmosphere. Each of these modes are empirically determined and not artificially constrained to have fixed amplitudes or frequencies. The fourth mode is shown to be consistently present and coherent throughout the troposphere. We further show that this mode is positively correlated with the solar cycle from 10 hPa down to the surface of the Earth over most of the globe. The statistical significance of this signal and its correlation with the 10.7-cm solar flux are established. We conclude that the atmosphere warms during the solar maximum almost everywhere over the globe. It should be pointed out that changes in the correlation values with latitude do not imply similar amplitude changes with latitude. However, the fact that the correlation with the solar flux is positive everywhere over the globe does imply that, on average, the temperatures increase during solar maxima at all latitudes. This makes the phenomenon difficult to explain with dynamical mechanisms involving overturning meridional circulations in the troposphere. This is useful information to atmospheric dynamicists wishing to come up with a mechanism for the influence of solar cycle variations on the lower atmosphere.

[12] **Acknowledgments.** We would like to kindly thank three anonymous reviewers of this paper for their useful comments. This research is supported by the National Science Foundation under grants DMS-0327658 and ATM-0332364.

References

Balachandran, N., and D. Rind (1995), Modeling the effects of UV variability and the QBO on the troposphere-stratosphere system. part I: The middle atmosphere, *J. Clim.*, *8*, 2058–2079.

Baldwin, M. P., and T. J. Dunkerton (1989), Observations and statistical simulations of a proposed solar cycle/QBO/weather relationship, *Geophys. Res. Lett.*, *16*, 863–866.

Coughlin, K. T., and K. K. Tung (2004), 11-year solar cycle in the stratosphere extracted by the empirical mode decomposition method, *Adv. Space Res.*, *34*, 323–329.

Crowley, T., and K.-Y. Kim (1996), Comparison of proxy records of climate change and solar forcing, *Geophys. Res. Lett.*, *4*, 359–362.

Dutton, E. G., and J. R. Christy (1992), Solar radiative forcing at selected locations and evidence for global lower tropospheric cooling following the eruptions of El Chichón and Pinatubo, *Geophys. Res. Lett.*, *19*, 2313–2316.

Frederick, J. (1977), Chemical response of the middle atmosphere to changes in the ultraviolet solar flux, *Planet. Space Sci.*, *25*, 1–4.

Gleisner, H., and P. Thejll (2003), Patterns of tropospheric response to solar variability, *Geophys. Res. Lett.*, *30*(13), 1711, doi:10.1029/2003GL017129.

Graf, H.-F., I. Kirchner, A. Robock, and I. Schult (1993), Pinatubo eruption winter climate effects: Model versus observations, *Clim. Dyn.*, *9*, 81–93.

Haigh, J. (1999), A GCM study of climate change in response to the 11-year solar cycle, *Q. J. R. Meteorol. Soc.*, *125*, 871–892.

Haigh, J. (2002), The effects of solar variability on the Earth's climate, *Philos. Trans. R. Soc. London, Ser. A*, *361*(1802), 95–111.

Hamilton, K. (1990), A look at the recently proposed solar-QBO-weather relationship, *J. Clim.*, *3*, 497–503.

Hershel, W. (1801), Observations tending to investigate the nature of the Sun, in order to find the causes or symptoms of its variable emission of light and heat, with remarks on the use that may possibly be drawn from solar observations, *Philos. Trans. R. Soc. London*, *91*, 265–318.

Huang, N. E., et al. (1998), The empirical mode decomposition and the hilbert spectrum for nonlinear and non-stationary time series analysis, *Proc. R. Soc. London, Ser. A*, *454*, 903–995.

Kalnay, E., et al. (1996), The NCEP/NCAR reanalysis 40-year project, *Bull. Am. Meteorol. Soc.*, *77*, 437–471.

Kodera, K. (1993), Quasi-decadal modulation of the influence of the equatorial quasi-biennial oscillation on the North Polar stratospheric temperatures, *J. Geophys. Res.*, *98*, 7245–7250.

Kuroda, Y., and K. Kodera (2002), Effect of solar activity on the polar-night jet oscillation in the Northern and Southern Hemisphere winter, *J. Meteorol. Soc. Jpn.*, *80*, 973–984.

Labitzke, K. (1982), On the interannual variability of the middle stratosphere during northern winter, *J. Meteorol. Soc. Jpn.*, *60*, 124–139.

Labitzke, K., and H. van Loon (1995), The 10–12 year oscillation: The solar cycle variation of the stratosphere, A STEP Working Group 5 report, 16 pp., Clim. and Global Dyn. Div., Nat. Cent. for Clim. Res., Boulder, Colo.

Labitzke, K., J. Austin, N. Butchart, J. Knight, M. Takahashi, M. Nakamoto, T. Nagashima, J. Haigh, and V. Williams (2002), The global signal of the

11-year solar cycle in the stratosphere: Observations and models, *J. Atmos. Sol. Terr. Phys.*, *64*, 203–210.

Lean, J., G. J. Rottman, H. L. Kyle, T. N. Woods, J. R. Hickey, and L. C. Puga (1997), Detection and parameterization of variations in solar mid- and near-ultraviolet radiation (200–400 nm), *J. Geophys. Res.*, *102*, 29,939–29,956.

Lee, H., and A. Smith (2003), Simulation of the combined effects of solar cycle, quasi-biennial oscillation, and volcanic forcing on stratospheric ozone changes in recent decades, *J. Geophys. Res.*, *108*(D2), 4049, doi:10.1029/2001JD001503.

McCormack, J., and L. Hood (1996), Apparent solar cycle variations of upper stratospheric ozone and temperature: Latitude and seasonal dependences, *J. Geophys. Res.*, *91*, 20,933–20,944.

Naito, Y., and I. Hirota (1997), Interannual variability of the northern winter stratospheric circulation related to the QBO and the solar cycle, *J. Meteorol. Soc. Jpn.*, *75*, 925–937.

Pittock, A. B. (1978), A critical look at long-term Sun-weather relationships, *Rev. Geophys.*, *16*, 400–420.

Ramanathan, V. (1988), The greenhouse theory of climate change: A test by inadvertent global experiment, *Science*, *240*, 293–299.

Rind, D., and J. Overpeck (1993), Hypothesized causes of decade-to-century-scale climate variability: Climte model results, *Quat. Sci. Rev.*, *12*, 357–374.

Salby, M., and P. Callaghan (2000), Connection between the solar cycle and the QBO: The missing link, *J. Clim.*, *13*, 2652–2662.

Shindell, D., et al. (1999), Solar cycle variability, ozone and the stratospheric circulation over northern Europe, *Science*, *284*, 305–308.

Soukharev, B. E. (1999), On the solar/QBO effect on the interannual variability of total ozone and the stratospheric circulation over northern europe, *J. Atmos. Sol. Terr. Phys.*, *61*, 1093–1109.

Soukharev, B. E., and L. L. Hood (2001), Possible solar modulation of the equatorial quasi-biennial oscillation: Additional statistical evidence, *J. Geophys. Res.*, *106*, 14,855–14,868.

Tett, S., P. Stott, M. Allen, W. Ingram, and J. Mitchell (1999), Causes of twentieth century temperature change near the Earth's surface, *Nature*, *399*, 369–372.

van Loon, H., and K. Labitzke (1998), The global range of the stratospheric decadal wave. part I: Its association with the sunspot cycle in summer and in the annual mean, and with the troposphere, *J. Clim.*, *11*, 1529–1537.

van Loon, H., and D. Shea (1999), A probable signal of the 11-year solar cycle in the troposphere of the Northern Hemisphere, *Geophys. Res. Lett.*, *26*, 2893–2896.

van Loon, H., and D. Shea (2000), The global 11-year solar signal in July–August, *Geophys. Res. Lett.*, *27*, 2965–2968.

Wetherald, R., and S. Manabe (1975), The effects of changing the solar constant of a general circulation model, *J. Atmos. Sci.*, *32*, 2044–2059.

Willson, R. C., and H. S. Hudson (1988), Solar luminosity variations in solar cycle-21, *Nature*, *332*(6167), 810–812.

K. Coughlin and K. K. Tung, Department of Applied Mathematics, University of Washington, Box 352420, Seattle, WA 98195, USA. (katie@amath.washington.edu)